EUROGRAPHICS 2016 / J. Jorge and M. Lin
(Guest Editors)

Volume 35 (2016), Number 2

A Multi-sided Bézier Patch with a Simple Control Structure

Tamás Várady[1] Péter Salvi[1] György Karikó[2]

[1] Budapest University of Technology and Economics
[2] ShapEx Ltd.

Abstract

A new n-sided surface scheme is presented, that generalizes tensor product Bézier patches. Boundaries and corresponding cross-derivatives are specified as conventional Bézier surfaces of arbitrary degrees. The surface is defined over a convex polygonal domain; local coordinates are computed from generalized barycentric coordinates; control points are multiplied by weighted, biparametric Bernstein functions. A method for interpolating a middle point is also presented.

This Generalized Bézier (GB) patch is based on a new displacement scheme *that builds up multi-sided patches as a combination of a base patch, n displacement patches and an interior patch; this is considered to be an alternative to the Boolean sum concept. The input ribbons may have different degrees, but the final patch representation has a uniform degree. Interior control points—other than those specified by the user—are placed automatically by a special degree elevation algorithm.*

GB patches connect to adjacent Bézier surfaces with G^1 continuity. The control structure is simple and intuitive; the number of control points is proportional to those of quadrilateral control grids. The scheme is introduced through simple examples; suggestions for future work are also discussed.

Categories and Subject Descriptors (according to ACM CCS): I.3.5 [Computer Graphics]: Computational Geometry and Object Modeling—Curve, surface, solid, and object representations

1. Introduction

The mathematical formulation of multi-sided surfaces is an important area in Computer Aided Geometric Design. There is a wide variety of these patches due to several (often contradictory) requirements, and it is hard to find a single best representation. For example, transfinite patches constrain only some boundaries and cross-derivatives, then the patch interior is created solely from this information. Control point-based patches provide multiple local controls for the interior by means of a well-defined structure of 3D vectors.

The transfinite approach is helpful when we are satisfied with the shape by the automatic settings, however, difficulties may arise if the shape needs to be further modified or optimized in the interior. Control point-based schemes are attractive when the number of control points is relatively low, however, if certain details at the boundaries require the presence of too many control points, it is hard to generate and manipulate these. Locality can be both an advantage and a problem, depending on whether we want to edit smaller or larger parts of the surface. Another aspect is how to stitch together adjacent surfaces smoothly; here transfinite patches may provide simpler solutions. The efficiency of numerical computations may also be a concern, and in this regard control point-based surfaces seem to be superior to transfinite surfaces, and the list goes on.

In this paper we propose a new control point-based surface representation, called the GB patch, which generalizes tensor product Bézier patches. It extends the mathematical elegance of Bézier patches to an arbitrary number of sides, and allows the combination of Bézier boundaries of different degrees with related cross derivatives. In some sense, we try to *combine* the advantages of the transfinite schemes (e.g. [SVR14]) and conventional control point-based approaches: basically the patch is constructed from boundary information, and at the same time an interior structure of control points is built up in an automatic manner. These control points may be satisfactory as they are, but can also be modified, allowing for interactive editing or shape optimization. The input Bézier ribbons may have different degrees and complexity, but each can be edited separately. The patch evolves naturally "behind the scenes", and smoothly blends together all information into a single entity. Interior control points are inserted when and where it is necessary.

Generalized Bézier patches are rational polynomials with C^∞ continuity within the patch. There is no need for artificial internal subdividing structures between quadrilaterals, however—according to our best knowledge—they cannot be directly converted into a standard CAD format. These patches can be utilized in various areas of CAGD: (i) Aesthetic design of complex free-form objects is still a challenging task; this includes general topology curve network-based design, as well. (ii) Hole filling is also an important problem in various modeling situations, in particular when complex vertex blends are created. (iii) The approximation of 3D

point clouds when points are located in an irregular, multi-sided region, is also an interesting application.

This paper is structured as follows. After reviewing previous work in Section 2, we discuss a new approach for creating multi-sided patches that applies the *displacement principle* (Section 3). We introduce the Generalized Bézier patch in Section 4 with its parameterization, control structure, and blending functions. In Section 5 the algorithm of combining Bézier surfaces of various degrees to constitute a single GB patch is discussed. This section comprises the algorithms of degree reduction and elevation for GB patches. The paper is concluded by a few examples (Section 6), including the pros and cons of the scheme and suggestions for future work.

2. Previous work

Multi-sided surfaces have been studied since the early 80s, see related reviews in [Mal98, VRS11] amongst others. An early control point-based solution appeared in Sabin's quadratic patch [Sab83], and the cubic surface of Hosaka and Kimura [HK84]. These were later generalized to arbitrary degrees by Zheng and Ball [ZB97] using a control net structure similar to ours. Their parameterization method depends on the number of sides; solutions for 3, 5 and 6-sided patches are described in the paper. The sum of the blending functions is set to 1 by compensating at the interior control points (cf. weight deficiency in our solution, see Section 4.4). The individual weights are products of powers of distance parameters, which yields an expression of much higher degree than the one proposed in Section 4.3. A subsequent publication [Zhe01] generalized this patch for non-twist-compatible configurations.

Another line of research started with the S-patch [LD89], where the binomial coefficients of Bernstein polynomials were replaced by multinomials, and the (u,v) quadrilateral domain was replaced by a convex polygon with generalized barycentric coordinates. While beautiful in theory, its practical use is somewhat limited due to the high number of control points and the special, fairly complex, multi-linked control structure. (For example, a 6-sided quintic S-patch requires 222 internal control points disregarding the boundaries; our GB patch only 25.) To our best knowledge, these problems have not been addressed, though a recent paper on cage deformation [SS15] proposes selective degree elevation for S-patches.

Warren [War92] introduced an interesting idea: multi-sided surfaces are created by "cutting off" edges of rational Bézier triangles, using *base points* (points where all homogeneous coordinates are 0). With this method, one can build patches of 3 to 6 sides with a low number of control points, and the boundary curves can have different degrees. C^1 continuity to adjacent patches can also be achieved, but this is not so straightforward, due to the special control structure (cf. Section 4.6).

A recent publication [SZ15] explores conditions for G^1 continuity between toric surfaces. This is a new and interesting multi-sided patch formulation, but the lattice structure of its control points is a constraint that may limit its usefulness for e.g. 5-sided surfaces.

None of the above publications deals with the automatic placement of control points. While this can arguably be done by minimizing a suitable target function, there is a strong demand in design applications to provide a default arrangement for the interior control points. Our solution for GB patches will be discussed in details in Section 5.

Finally we should mention a special kind of n-sided patches, that are created as a collection of rectangular patches with central splitting. The main issues are how to create and control good subdividing boundaries, and how to ensure smooth connections between the adjacent patches, in particular at the extraordinary center point. We can list only a few from the many interesting publications. One of the earliest was Gregory's C^1 bicubic solution [GZ94], followed by various biquadratic, bicubic and biquartic surface splines with G^1 (e.g. [Pet94]), biseptic with G^2 [LS08], and bisextic surfaces with C^2 continuity [Pra97]. A recent result in this area is a fair, quasi-G^2 continuous biquartic configuration proposed in [KNP15].

The basic advantage of these methods is that they stitch together standard patches, but may not have high-degree continuity along their seam lines, in contrast to genuine n-sided patches, such as the GB patch. Another aspect is that the majority of these methods approximate a control polyhedron, while our focus is to develop a combined scheme that interpolates a prescribed set of curves and offer additional interior control.

In the forthcoming sections we will discuss several features that distinguish the proposed GB scheme from other approaches, such as: simple control structure, ease of connecting multiple ribbons with various degrees, intuitive method to automatically generate interior control points (gaining further degrees of freedom), and C^∞ continuity in the interior of the patch.

3. The displacement approach

The majority of transfinite patch formulations for quadrilateral and n-sided patches are based on the Boolean sum principle. Bicubic Coons patches [Coo67] take two side-to-side interpolants and subtract a correction term that interpolates the corner positions, tangents, and twists. Gregory patches [Gre86] use corner interpolants, where the sum of two adjacent boundaries and cross-derivatives is compensated by correction terms. Generalized Coons patches, proposed in [SVR14], are also composed by adding n side ribbons and subtracting n corner correction terms to ensure interpolation along the boundaries.

Here we propose an alternative, the *displacement* scheme. The basic idea is that we define curves by separating the end constraints (positions and first derivatives) from their middle parts. For surfaces we distinguish three parts: corner constraints (positions, tangents and twists), side constraints (positions and cross-derivatives), and a surface interior. We will use this approach for combining Bézier surfaces using GB patches.

Any parametric curve can be written as $r(u) = r_B(u) + r_D(u)$, where $r_B(u)$ denotes the *base* curve, and $r_D(u)$ denotes the *displacement* curve. We assume that $r_B(u)$ interpolates the end positions and end tangents, i.e., (assuming a parametric interval of $[0,1]$) $r_B(0) = r(0)$, $r_B(1) = r(1)$, $r'_B(0) = r'(0)$, $r'_B(1) = r'(1)$. Let us take a simple example, see Figure 1. A quartic Bézier curve

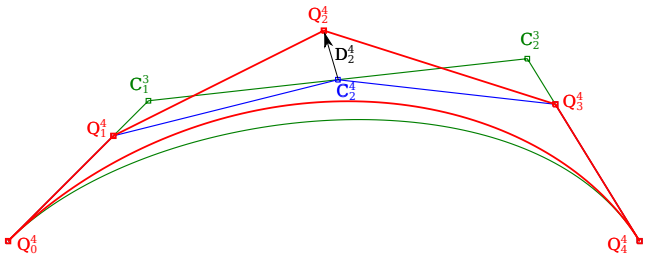

Figure 1: Displacements (red: original quartic curve, green: cubic curve, blue: cubic curve elevated to quartic).

is given as

$$r(u) = \sum_{i=0}^{4} Q_i^4 B_i^4(u), \tag{1}$$

where Q_i^4 are its control points. The base curve $r_B(u)$ is a cubic curve

$$r_B(u) = \sum_{i=0}^{3} C_i^3 B_i^3(u), \tag{2}$$

where $C_0^3 = Q_0^4$, $C_1^3 = Q_0^4 + \frac{4}{3}(Q_1^4 - Q_0^4)$, $C_2^3 = Q_4^4 + \frac{4}{3}(Q_3^4 - Q_4^4)$, and $C_3^3 = Q_4^4$.

After degree elevating $r_B(u)$, an identical curve of degree 4 is obtained with control points C_i^4. Clearly $C_i^4 = Q_i^4$, except for $i = 2$; where $C_2^4 = \frac{1}{2}(C_1^3 + C_2^3) \neq Q_2^4$. We define the displacement vector D_2^4 between the middle control points as $D_2^4 = Q_2^4 - C_2^4$, and thus obtain a displacement curve $r_D(u) = D_2^4 B_2^4(u)$. It can be seen that $r_D(u)$ influences only the middle part of the curve and not the ends.

The same logic can be applied to n-sided surfaces, as well. Let us compose our surface as the sum of a base patch, n displacement patches and an interior patch:

$$S(u,v) = S_B(u,v) + \sum_{i=1}^{n} S_{D_i}(u,v) + S_I(u,v). \tag{3}$$

The base patch interpolates the corner data, the displacement patches act only in the middle of the sides and vanish as we move towards the corners. The interior patch determines the surface in the middle and vanishes as we approach the sides and the corners.

While in the Boolean sum approach correction terms are subtracted, in the displacement approach the sum of different surface components are taken. By switching the individual components "on" and "off", local effects can be observed and analyzed.

4. The Generalized Bézier patch

A Generalized Bézier (GB) patch $S(u,v)$ is generated by mapping the (u,v) points of an n-sided convex polygonal domain Γ into 3D. We can handle patches with an arbitrary number of sides ($n \geq 3$). The sides of the polygon Γ_i ($i = 1 \ldots n$) are mapped to the boundaries of the patch; each boundary is a degree d Bézier curve. The multi-sided control net, whose structure is determined by n and d, is a straightforward extension of the control grid of quadrilateral Bézier patches with degree d.

We associate certain rows of control points with individual sides of the domain and introduce the number of control point layers $l = (d+1) \div 2$. For example, Figure 4 shows a 5-sided, degree 4 control net where $l = 2$. Figure 5 shows a 5-sided, degree 5 control net where $l = 3$. (From the above definition it follows that there are always two patches with a given number of layers, with degree $d = 2l$ and $d = 2l - 1$.)

First we introduce some elements of the GB scheme, including control net, parameterization and weight deficient blending functions, and then we will be able to formulate the surface equation.

4.1. Control nets

The concept of multi-sided control nets is depicted in Figure 2. First let us consider a quadrilateral control grid. For even degrees the grid consists of a central control point and four *quadrants* (black frames in Fig. 2a). For odd degrees (see Fig. 2b) a conventional grid consists of just the four quadrants. It is a peculiar feature of the GB patch, that its control network contains a central control point (C_0) also for odd degrees. This structure can be generalized to n corners; the number of control points will be proportional to n.

Comparing the above examples with the five-sided patches of Figures 2c and 2d, we can see that in the quartic case, the 4-sided patch has $4 \cdot 6 + 1 = 25$ control points, while the 5-sided GB patch has $5 \cdot 6 + 1 = 31$ points. In the quintic case, a conventional 4-sided patch (with no C_0) has $4 \cdot 9 = 36$ control points, while the 5-sided GB patch has $5 \cdot 9 + 1 = 46$ points.

In general, for even degrees ($d = 2l$), the number of control points is $n \cdot l(l+1) + 1$ for both the conventional 4-sided and the n-sided GB patches. For odd degrees ($d = 2l - 1$), the number of control points is $4l^2$ for the conventional 4-sided patches, and $n \cdot l^2 + 1$ for the n-sided GB patches.

4.2. Local coordinates and Bernstein blending functions

For each side of the polygonal domain we introduce local side and distance parameters, denoted by $s_i = s_i(u,v)$ and $h_i = h_i(u,v)$, see Figure 3. These parameters are computed using Wachspress barycentric coordinates $\lambda_i = \lambda_i(u,v)$, $i = 1 \ldots n$. There are several publications that thoroughly discuss the properties of generalized barycentric coordinates, see for example [HF06]. It is well-known that (i) $\lambda_i \geq 0$ [positivity] and (ii) $\sum \lambda_i = 1$ [partition of unity] hold for all points within a convex domain. Denote the vertices of the polygon by P_i and take an arbitrary point (u,v). Then (iii) $(u,v) = \sum P_i \lambda_i(u,v)$ [reproduction] holds, as well. Finally, for all vertices P_j, we have (iv) $\lambda_i = \delta_{ij}$ [Lagrange property], where δ_{ij} is the Kronecker delta.

While generalized barycentric coordinates are associated with the vertices of the polygon, the s_i and h_i parameters of GB patches are associated with the individual sides, inheriting important properties that we will use later.

Let us define the local parameters as

$$s_i = \frac{\lambda_i}{\lambda_{i-1} + \lambda_i}, \tag{4}$$

$$h_i = 1 - \lambda_{i-1} - \lambda_i. \tag{5}$$

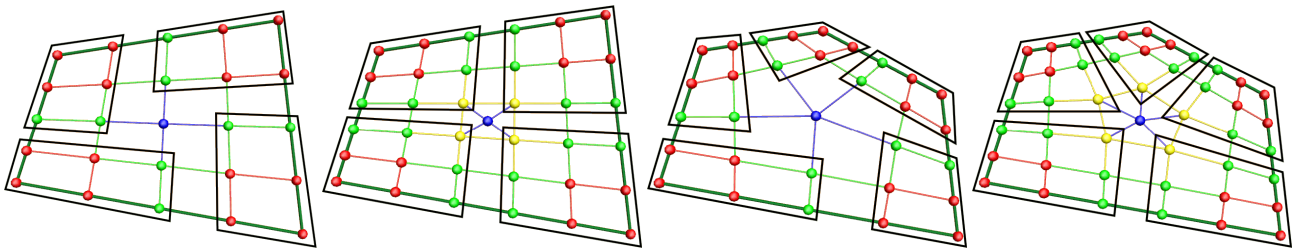

(a) $n = 4, d = 4$ (b) $n = 4, d = 5$ (c) $n = 5, d = 4$ (d) $n = 5, d = 5$

Figure 2: Quadrants of quartic and quintic patches.

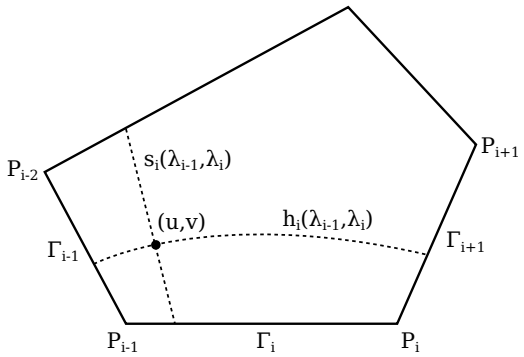

Figure 3: Multi-sided domain and parameterization.

The side parameter s_i varies from 0 to 1 on side i; $s_i = 0$ on side $i-1$, $s_i = 1$ on side $i+1$. For all other points, s_i takes values between 0 and 1. The distance parameter h_i vanishes on side i, since this is the only place where the sum $\lambda_{i-1} + \lambda_i$ equals to 1. It increases linearly from 0 to 1 on sides $i-1$ and $i+1$. On the remaining sides $h_i = 1$. On side i the equations $s_i = h_{i-1}$ and $s_i = 1 - h_{i+1}$ are also satisfied.

Note: the above equation for s_i is undefined for points on the "distant" sides Γ_j, $j \notin \{i-1, i, i+1\}$, however, there exists an equivalent formula that resolves this problem. Introducing $h^{\perp}_{i-1}$ and $h^{\perp}_{i+1}$ as the perpendicular distances from edges Γ_{i-1} and Γ_{i+1}, we have

$$s_i = \frac{\sin(\theta_i) h^{\perp}_{i-1}}{\sin(\theta_i) h^{\perp}_{i-1} + \sin(\theta_{i-1}) h^{\perp}_{i+1}}, \tag{6}$$

where θ_i denotes the angle at P_i.

We are going to use degree d biparametric Bernstein blending functions of (s_i, h_i) over the domain:

$$B^d_{j,k}(s_i, h_i) = \binom{d}{j} (1-s_i)^{d-j} s_i^j \cdot \binom{d}{k} (1-h_i)^{d-k} h_i^k. \tag{7}$$

These Bernstein functions are defined in the same way as for the quadrilateral domains with the difference that the "opposite" side (where $h_i = 1$) will be mapped to multiple sides of the domain polygon.

4.3. Control points of the i-th side

The control points of the i-th side are denoted by $C^{d,i}_{j,k}$, $0 \le j \le d$, $0 \le k < l$. The "contribution" of the i-th side can be written as

$$S^d_i(s_i, h_i) = \sum_{j=0}^{d} \sum_{k=0}^{l-1} \mu^i_{j,k} C^{d,i}_{j,k} B^d_{j,k}(s_i, h_i). \tag{8}$$

The $\mu^i_{j,k}$-s are scalar multipliers that will ensure that the multi-sided patch on side i is determined *solely* by its associated control points $C^{d,i}_{j,k}$. In other words, neither the adjacent, nor the distant sides will have any effect on the i-th side.

It is important to notice that there are *shared* control points around the corners that affect *two* adjacent sides. For example, take the four control points (colored red) in Figure 4 that fall into both the black and grey frames. These four control points determine the position, the first derivatives and the mixed partial derivative (twist vector) of the patch at the corner. (For simplicity's sake we assume twist compatibility in this paper.) Taking the bottom side as side i, these control points occur both in the $S^d_i(s_i, h_i)$ and $S^d_{i+1}(s_{i+1}, h_{i+1})$ parts, being indexed in two different ways. For the i-th side we have $C^{d,i}_{j,k}$, $j \in \{d-1, d\}$, $k \in \{0,1\}$; for the $(i+1)$-th side $C^{d,i+1}_{j,k}$, $j,k \in \{0,1\}$. This also means that in the final surface equation the shared control points will actually be multiplied by a weighted combination of Bernstein functions

$$\mu^i_{d-k,j} B^d_{d-k,j}(s_i, h_i) + \mu^{i+1}_{j,k} B^d_{j,k}(s_{i+1}, h_{i+1}), \quad j,k \in \{0,1\}.$$

In Figure 4 a quartic patch is shown ($l = 2$) with quadruples of shared control points. In Figure 5 a quintic patch is shown ($l = 3$), where 3×3 control points are shared at each corner.

Let us return to assigning weights to the control points of the i-th side. First take the quartic case in Figure 4. The four shared control points at the left will be multiplied by a scalar function α_i, and those at the right by β_i (see below). A weight of 1 will be assigned to the control points in the middle. Formally, we define $\mu^i_{j,k}$ as

$$\mu^i_{j,k_{<2}} = \begin{cases} \alpha_i = \frac{h_{i-1}}{h_{i-1}+h_i} & j < 2, \\ 1 & 2 \le j \le d-2, \\ \beta_i = \frac{h_{i+1}}{h_{i+1}+h_i} & j > d-2. \end{cases} \tag{9}$$

This sets all μ-s to 1 on the i-th side, where $h_i = 0$, thus producing a constant 1 multiplier for the corresponding Bernstein functions.

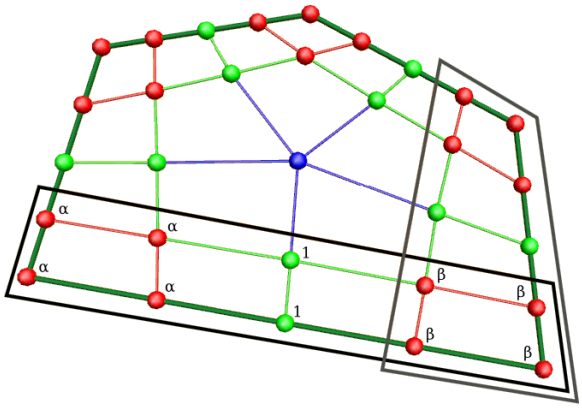

Figure 4: Control points of a patch with 2 layers ($n = 5$, $d = 4$).

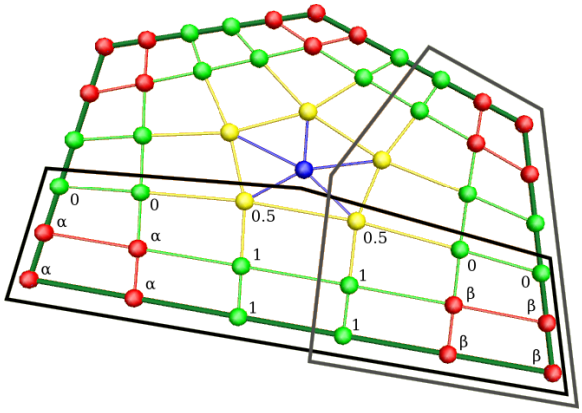

Figure 5: Control points of a patch with 3 layers ($n = 5$, $d = 5$).

The method of assigning weights is more complicated when $l \geq 3$; an example is shown in Figure 5. All weights for $k < 2$ are computed as before. When $k \geq 2$, take the diagonal $j = k$ on the left side (where $j < l$). Weights of $\frac{1}{2}$ will be assigned to the control points on the diagonal, and zeros for all the control points above this diagonal (where $j < k$). Taking the right side, another diagonal is defined by $j = d - k$; the weights are assigned in a similar manner as before. All the remaining weights of the control points between the two diagonals belong exclusively to the i-th side and will have a weight of 1. We can formally define the $k \geq 2$ case as follows:

$$\mu^i_{j,k} \underset{j<l}{=} \begin{cases} 0 & j < k, \\ \frac{1}{2} & j = k, \\ 1 & j > k, \end{cases} \qquad \mu^i_{j,k} \underset{j\geq l}{=} \begin{cases} 0 & j > d-k, \\ \frac{1}{2} & j = d-k, \\ 1 & j < d-k. \end{cases} \tag{10}$$

4.4. Weight deficiency

For affine invariance the sum of the blending functions must be 1. In the case of GB patches, we introduce a central control point that is multiplied by a central blending function $B^d_0(u,v)$, that is equal to the weight deficiency of the blending functions assigned to the other control points:

$$B^d_0(u,v) = 1 - \sum_{i=1}^{n} \sum_{j=0}^{d} \sum_{k=0}^{l-1} \mu^i_{j,k} B^d_{j,k}(s_i(u,v), h_i(u,v)). \tag{11}$$

We have found that setting the default center point to the average of the n innermost control points is a natural choice:

$$C_0 = \frac{1}{n} \sum_{i=1}^{n} C^{d,i}_{l,l-1}. \tag{12}$$

With this we can define an interior surface using the central control point as

$$S^d_0(u,v) = C_0 B^d_0(u,v). \tag{13}$$

The central control point is useful for moving the middle point of the GB patch to an arbitrary location, as we will see in Section 5.3.

4.5. The patch equation

Now we are ready to formulate the equation of the GB patch. Using Equations (8) and (13):

$$S^d(u,v) = \sum_{i=1}^{n} S^d_i(s_i(u,v), h_i(u,v)) + S^d_0(u,v). \tag{14}$$

The GB patch is a convex combination of a net of control points, similarly to the tensor product Bézier patches. As shown in Figure 6, the control points can be classified by their location within the structure. Control points around the vertices (red) are to reproduce the positional and tangential constraints at the corners; these are multiplied by a rational combination of two biparametric Bernstein functions. Control points between these quadruples (green) are to reproduce boundaries and cross-derivatives; control points in the interior (yellow) are to produce a smooth blend between the boundaries and the interior. The latter groups of control points are multiplied by ordinary biparametric Bernstein functions. Finally, the central control point (blue) is to adjust the interior of the GB patch, and is multiplied by a special blend, the weight deficiency.

In the next subsection we will investigate how GB patches can be connected to adjacent tensor product Bézier surfaces or other GB patches with G^1 continuity.

4.6. Bézier ribbons and cross-derivatives

Let us take the first two rows of control points that belong to side i: $C^{d,i}_{j,k}$, $k < 2$. Using ordinary biparametric Bernstein functions, these define a *Bézier ribbon*, that determines a boundary curve r^d_i and a first cross-derivative t^d_i along the side parameter s_i:

$$r^d_i(s_i) = \sum_{j=0}^{d} C^{d,i}_{j,0} B^d_{j,0}(s_i, 0), \tag{15}$$

$$t^d_i(s_i) = \sum_{j=0}^{d} d(C^{d,i}_{j,1} - C^{d,i}_{j,0}) B^d_{j,0}(s_i, 0). \tag{16}$$

Let us take the same set of control points and apply the local parameterization and the weighted Bernstein functions of GB patches. We will show that $S(u,v)$ and $S'(u,v)$ reproduces the boundary and

the cross-derivative along Γ_i. In this section x' denotes a directional derivative of x by an arbitrary direction in the (u,v) domain. Our proof consists of three parts. First we show that $S_i(u,v)$ does not affect the distant sides Γ_j, $j \notin \{i-1,i,i+1\}$, neither in positional nor in differential sense. Then we show how $S_i(u,v)$ affects the adjacent sides Γ_j, $j \in \{i-1,i+1\}$. Finally we show that $S_i(u,v)$ reproduces the prescribed boundary functions. For this proof, it is sufficient to investigate the properties of the weighted Bernstein functions $\mu^i_{j,k}B^d_{j,k}(s_i,h_i)$ and their derivatives $\left(\mu^i_{j,k}B^d_{j,k}(s_i,h_i)\right)'$ in the first two rows ($k<2$).

(i) The contribution of Γ_i does not affect the distant sides, since the weighted Bernstein functions and their derivatives vanish. This holds, because by definition h_i equals 1 there, and all related blending functions contain a $(1-h_i)^2$ term.

(ii) Take the positional contributions of Γ_i to the adjacent side Γ_{i-1}. (For Γ_{i+1} we proceed in the same way.) The weighted Bernstein functions vanish, since (a) for $j<2$ the multiplier $\mu^i_{j,k}=0$ due to $h_{i-1}=0$, (b) the remaining Bernstein functions with $j\geq 2$ contain at least one s_i term, but $s_i=0$ on side Γ_{i-1}.

Next look at the derivatives of the weighted Bernstein functions of Γ_i on Γ_{i-1}. Those with indices $j\geq 2$ have obviously no effect on Γ_{i-1}, as they contain at least one s_i term, and $s_i=0$. But for $j<2$ the derivatives do contribute to Γ_{i-1}:

$$\left(\frac{h_{i-1}}{h_{i-1}+h_i}B^d_{j,k}\right)' = \frac{h'_{i-1}}{h_i}B^d_{j,k}(s_i,h_i). \tag{17}$$

Similarly, the contribution to the other side (Γ_{i+1}) is

$$\left(\frac{h_{i+1}}{h_{i+1}+h_i}B^d_{j,k}\right)' = \frac{h'_{i+1}}{h_i}B^d_{j,k}(s_i,h_i). \tag{18}$$

(iii) The related boundary curve will be reproduced positionally on Γ_i, since the ordinary and weighted Bernstein functions become identical. For $2\leq j\leq d-2$ all $\mu^i_{j,k}$-s are constant 1; for the corner terms, where $j<2$ or $j>d-2$ the $\mu^i_{j,k}$-s are also equal to 1, since $h_i=0$, see Eq. (9).

In order to show the reproduction of the cross-derivative function, we need to show that the derivatives of the weighted Bernstein functions are identical to those of the ordinary Bernstein functions. We will take into consideration the differential terms from the Γ_{i-1} and Γ_{i+1} sides. First take the left corner, where

$$\left(\frac{h_{i-1}}{h_{i-1}+h_i}B^d_{j,k}\right)' = B^d_{j,k}(s_i,h_i)' - \frac{h'_i}{h_{i-1}}B^d_{j,k}(s_i,h_i), \tag{19}$$

while the contribution from the $(i-1)$-th side is

$$\frac{h'_i}{h_{i-1}}B^d_{d-k,j}(s_{i-1},h_{i-1}), \tag{20}$$

as can be seen by shifting the indices of Eq. (18). When $h_i=0$, all coefficients vanish except for $B^d_{j,0}(s_i,h_i)$ and $B^d_{d,j}(s_{i-1},h_{i-1})$. Fortunately $h_i=1-s_{i-1}=0$ and $s_i=h_{i-1}$ on the i-th boundary, consequently

$$B^d_{j,0}(s_i,h_i) = B^d_{d,j}(s_{i-1},h_{i-1}), \quad j<2. \tag{21}$$

This means that the contribution from Γ_{i-1} cancels the second term of Eq. (19), and only $B^d_{j,k}(s_i,h_i)'$ remains, this is exactly what we wanted to prove. The same cancellation takes place at the other corner due to the contribution from side Γ_{i+1}.

To sum it up, we have shown that the weighted Bernstein functions of $S(u,v)$ are identical to the ordinary Bernstein functions on Γ_i along the boundary, i.e., the GB patch behaves as an ordinary Bézier patch having the same two rows of control points. Thus GB patches can be inserted into patchworks of quadrilateral Bézier patches, and they can be smoothly connected to other multi-sided GB patches.

5. Control network generation

In this section we will discuss how Generalized Bézier patches can be used to interpolate and nicely blend Bézier ribbons of different degrees into a single multi-sided patch. We will show how the individual ribbons can be degree elevated preserving the boundary constraints, and how new control points can be inserted in the interior to complete the patch. These algorithms generalize the degree reduction and elevation algorithms of Bézier curves.

5.1. Degree elevation and reduction

The algorithm to degree elevate Bézier curves is well-known. Take a degree d control polygon with control points C^d_i, $i=0\ldots d$. Keep the end control points $C^{d+1}_0=C^d_0$ and $C^{d+1}_{d+1}=C^d_d$, and create new interior control points on each chord of the polygon by linear interpolation: $C^{d+1}_i=\eta_i C^d_{i-1}+(1-\eta_i)C^d_i$, where $\eta_i=\frac{i}{d+1,}$, $i=1\ldots d$. The new curve will be a convex combination of control points using the B^{d+1}_i Bernstein functions.

Concerning the degree reduction of Bézier curves there are different possibilities. Our preference is to perform an "inverse" degree elevation. In the elevation process, we have d equations to determine d unknowns, while in reduction we use the same equations to determine the unknown internal control points C^d_i, $i=1\ldots d-1$ from the given C^{d+1}_i-s, but here we have one more equation than needed. Using index i upwards from 1, and j downwards from d we obtain the following pairs of equations:

$$C^d_i = \frac{C^{d+1}_i-\eta_i C^d_{i-1}}{1-\eta_i}, \qquad 1\leq i\leq k, \tag{22}$$

$$C^d_{j-1} = \frac{C^{d+1}_j-(1-\eta_j)C^d_j}{\eta_j}, \qquad d-k+1\leq j\leq d, \tag{23}$$

where $k=d\div 2$. We have $2k$ equations and $d-1$ unknowns, so for $d=2k+1$ these are sufficient to determine all the interior control points, but for $d=2k$ we obtain two different expressions for C^d_k, and their average needs to be taken.

Degree elevation is trivial for quadrilateral Bézier patches and relatively easy for GB patches, as well, generalizing the above algorithm. We retain the corner control points, and degree elevate the boundaries by inserting new control points to each chord of the perimeter control polygons; then for each quadrilateral of the control net we insert a new control point by linear interpolation. For the GB patches it is essential that the central control point can also act as a corner of a quadrilateral, so it does influence the degree

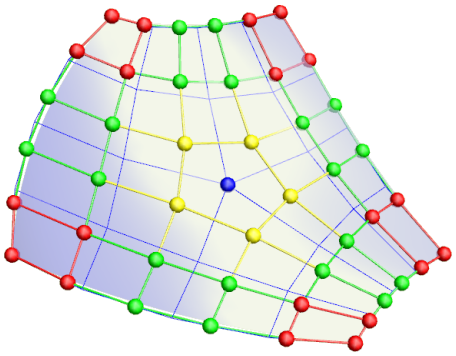

Figure 6: Degree elevation from quartic to quintic—blue lines show the original control net. Control points are colored by classification (see Section 4.5).

elevation process. This is illustrated in Figure 6, where a quintic control net was created from a quartic.

Degree elevation for GB patches basically proceeds as for quadrilateral patches. Assume we have a patch with l layers, then

$$C_{j,k}^{d+1,i} = \eta_j \vartheta_k C_{j-1,k-1}^{d,i} + (1-\eta_j)\vartheta_k C_{j,k-1}^{d,i} + \eta_j(1-\vartheta_k) C_{j-1,k}^{d,i} + (1-\eta_j)(1-\vartheta_k) C_{j,k}^{d,i}, \quad (24)$$

where $\eta_j = \frac{j}{d+1,}$, $\vartheta_k = \frac{k}{d+1,}$, $1 \le j \le l$, $1 \le k \le d \div 2$.

There are two options for setting the central control point C_0^{d+1}: either we compute the default central point, as was proposed in Equation (12), or we compute C_0^{d+1} in such a way, that the middle surface point stays the same. Details of the latter approach can be found in Section 5.3. We are going to use the following notation for the degree elevation operation: $S^{d+1}(u,v) = \left[S^d(u,v)\right]^{\uparrow}$.

It must be emphasized that degree elevation does not produce an identical GB surface, as in the case of tensor product Bézier patches. The above procedure creates an elevated network, but the weights of the control points are computed as it was described in Section 4.3. The boundaries and cross-derivatives are preserved, of course, but the interior of the elevated patch only approximates the original patch. This is due to the different blending functions and the different weight deficiencies. Figure 7a shows a 6-sided quintic patch, and Figure 7b shows its degree elevated version with a superimposed deviation map. There are minor differences, even when the middle point of the surfaces are kept identical.

Degree reduction for GB patches is also fairly straightforward, based on the related curve algorithm, so we do not go into details, just introduce a notation: $S^d(u,v) = \left[S^{d+1}(u,v)\right]^{\downarrow}$.

5.2. Creating a GB patch from Bézier ribbons

The input is a collection of Bézier ribbons with different degrees, denoted by d_i, $i = 1 \ldots n$, see for example Figure 8a. We are going to create a GB patch of degree $d_{\max} = \max(d_i)$, that interpolates and smoothly connects these ribbons. The patch will have a well-defined net of internal control points, along with a central control

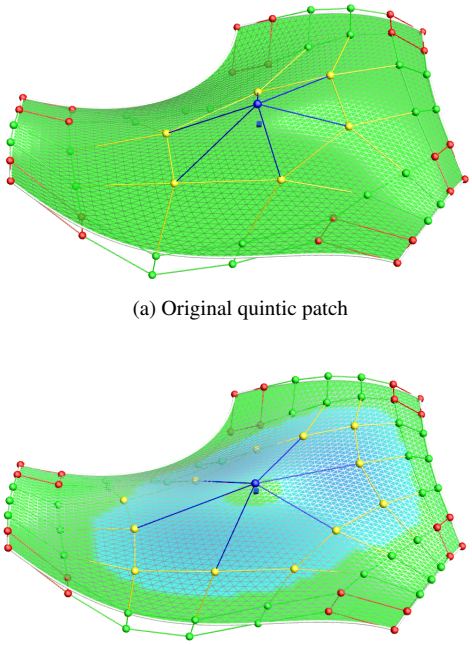

(a) Original quintic patch

(b) Sextic patch with deviation

Figure 7: Deviations after elevation.

point. All control points can be used for editing or optimization. The algorithm is split into three phases.

(i) In the first phase we reduce the degrees of the individual ribbons step by step from d_i to 3. Using our former notations, the control points of the i-th ribbon are $C_{j,k}^{d_i,i}$, $j = 0 \ldots d_i$, $k < 2$. After the first degree reduction we obtain $C_{j,k}^{d_i-1,i}$, $j = 0 \ldots d_i - 1$, $k < 2$; then at the end $C_{j,k}^{3,i}$, $j = 0 \ldots 3$, $k < 2$. (Intermediate control points are stored for later use.)

(ii) We create a base patch $S^3(u,v)$, defined by n quadruples of control points, associated with the corners. We assume that the ribbons are compatible, i.e., although their degrees may be different, they must define the same position, tangents and twist vectors at the corners. Consequently, after the degree reduction phase is completed, a consistent cubic control net with cubic boundaries and cross-derivatives is obtained. We set the central control point C_0^3 (see Section 5.3) and start to build the network bottom up.

(iii) We perform degree elevations step by step for each side and create intermediate surfaces $M^d(u,v)$. First we compute $M^4(u,v) = \left[S^3(u,v)\right]^{\uparrow}$; the degree elevated control points of the i-th ribbon are denoted by $Q_{j,k}^{4,i}$. Then we compute the displacement vectors for all ribbons whose degree was at least 4. These vectors will compensate the corresponding control points of the current intermediate surface to reproduce all degree 4 ribbons, or partly reproduce ribbons with degrees greater then 4. Finally we compute the degree 4 interior control points.

In general, we repeat this step several times: intermediate sur-

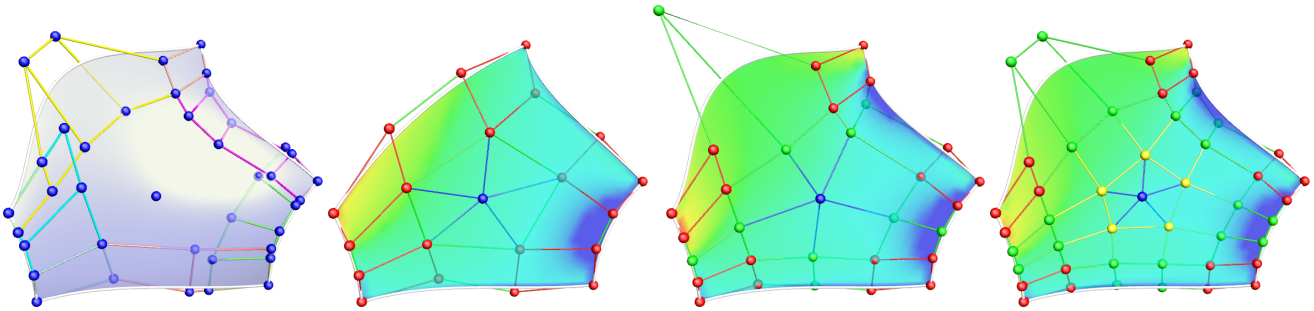

(a) Input Bézier ribbons (b) Reduced to cubic (base patch) (c) Elevated to quartic (d) Elevated to quintic (final patch)

Figure 8: Evolution of a GB patch.

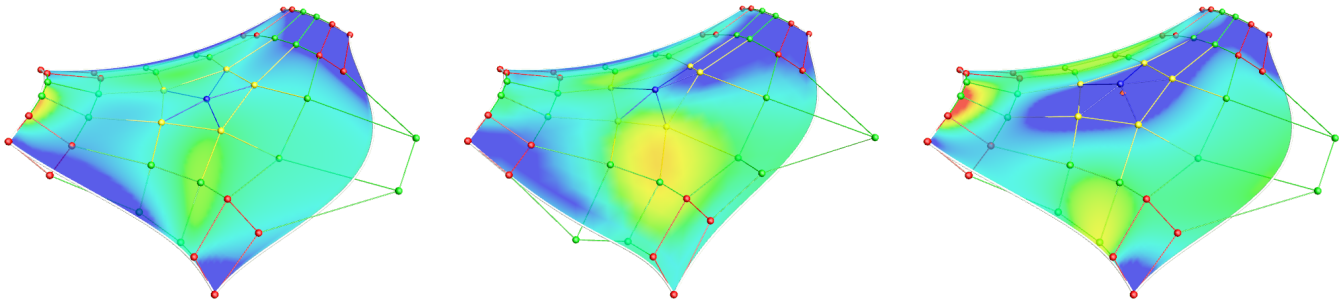

(a) Initial configuration (b) Moving control points (c) Moving the surface center

Figure 9: Editing a GB patch.

faces are computed as $M^d(u,v) = \left[S^{d-1}(u,v)\right]^{\uparrow}$, then displacement corrections are made where $C^{d,i}_{j,k}$ exists and the difference vectors $C^{d,i}_{j,k} - Q^{d,i}_{j,k}$, $j = 2 \ldots d_i$, $k < 2$ are not zero. Obviously, we never tweak the default quadruples at the corners, since they are always properly set. Then we define C^d_0, and this completes the patch $S^d(u,v)$. After repeated degree elevations the process terminates at the highest degree $d_{\max}$.

The evolution of the GB patch is demonstrated by a simple example in Figure 8. Figure 8a shows a patch with five ribbons with degrees 3, 4, 5, 5, and 3, respectively, starting at the bottom edge and going in CCW direction. After degree reductions we obtain the base patch with boundaries reduced to cubic (Figure 8b). The first degree elevation retains the shape of ribbons 1 and 5, reproduces the quartic ribbon 2, and modifies ribbons 3 and 4 (Figure 8c). The second degree elevation retains the shape of ribbons 1, 2 and 5, and reproduces the quintic ribbons 3 and 4. Figure 8d shows the final quintic patch with its automatically inserted interior control points, which ensure a natural blending to connect the input ribbons.

5.3. Computing the central control point

An alternative method for computing the central control point C_0 allows one to specify a 3D point P_0 to be interpolated by the middle point of the surface. Let (u_0, v_0) denote the center of the domain polygon, then we want to set $S^d(u_0, v_0) = P_0$. Using Equations (13) and (14) we can reformulate this as

$$\sum_{i=1}^{n} S^d_i(s_i(u_0,v_0), h_i(u_0,v_0)) + C_0 B^d_0(u_0,v_0) = P_0, \qquad (25)$$

from which we can compute C_0 as

$$C_0 = \frac{P_0 - \sum_{i=1}^{n} S^d_i(s_i(u_0,v_0), h_i(u_0,v_0))}{B^d_0(u_0,v_0)}. \qquad (26)$$

6. Evaluation

In this section we will present a few examples and discuss the strengths and weaknesses of the GB patch.

6.1. Example 1

The control points of GB patches can be manually edited or optimized as in standard control point-based formulations. Figure 9a shows the curvature map of a 5-sided patch, whose control points—both in the interior and along the boundaries—have been modified; see Figure 9b. (Computing derivatives in the interior is possible, but quite complex, and thus the curvature maps here were computed using a dense triangular mesh.) The user may want to explicitly set the middle surface point to adjust the fullness of the shape. Then degree elevation will proceed accordingly, and in each phase an appropriate central control point will be set to satisfy this additional

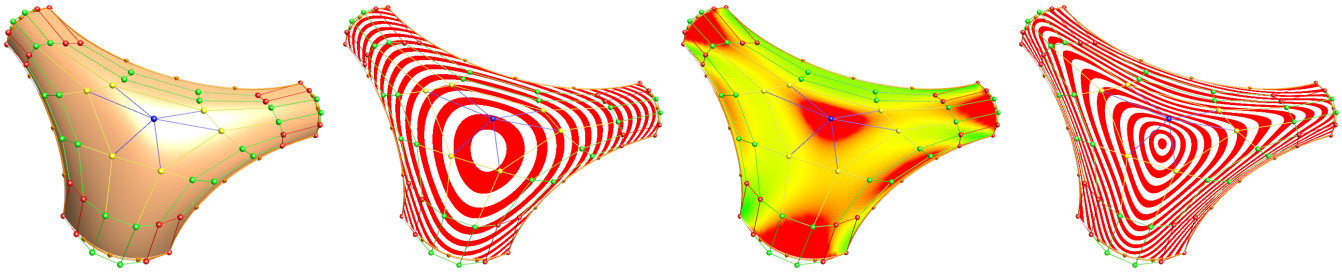

(a) Control points (b) Contouring (c) Gaussian curvature (d) Isophote lines

Figure 10: A setback vertex blend.

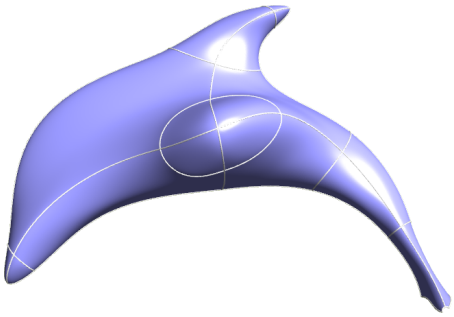

Figure 11: The dolphin model.

constraint. The result is shown in Figure 9c, where the first two layers of the control points are the same as before, but the interior and central control points are relocated to force the surface to interpolate the small red cubical marker in the middle.

6.2. Example 2

GB patches are well-suited for creating vertex blends. For example, Figure 10 shows a 6-sided setback-type vertex blend, which connects three edge blends with different radii. The boundary constraints are determined by the surrounding primary and fillet surfaces, and the fullness of the patch is also optimized by means of the interior control points.

6.3. Example 3

GB patches can be used to fill up general topology curve networks. The degree of the ribbons associated with the edges of the network may be different, but for smooth surfaces it is necessary that the twist vectors should be compatible at the corners and G^1 continuity is ensured between the ribbons sharing the same edge. Then the GB patches will automatically provide G^1 transitions, as well. A dolphin model is shown in Figures 11–13. It consists of 12 curves that define eighteen faces: eight 3-sided, four 4-sided, four 5-sided and two 6-sided surface patches. Some close-up pictures show the top-left 6-sided patch with its ribbons (12a), full control-net (12b) and isophotes (12c). Another close-up sequence shows six patches together with ribbons (13a), mean curvature map (13b) and slicing (13c).

6.4. Example 4

The woman head in Figure 14 is a fairly complex surface model with many details, including the eyes, the nose and the ears. Altogether there are 117 curves that define 105 patches. Besides several 6-sided and 3-sided patches, the important large areas are dominantly covered by 4-sided and 5-sided patches. This model was created as a collection of Generalized Bézier patches; a 5-sided patch—with its control-net—is shown in the middle.

6.5. Advantages/limitations and future work

The simplicity of the control structure is an attractive feature of GB patches. Control points can be defined by means of external layers, then the proposed method fills up the internal control points in a fair and predictable manner, and these can be further edited, as well. The setting of the central control point is not an obvious issue. Our proposed default setting (see Section 4.4) is one possibility, but alternative solutions may also exist.

The GB patch inherits important properties of ordinary Bézier patches, including affine invariance (see notes below), convex hull property, linear reproduction and localized effect of editing. Our high-resolution numerical tests ($n = 4 \dots 12$, $d = 3 \dots 12$) meet the expectations that weight deficiency is always positive. Unfortunately, at this point we have no algebraic proof, and this is subject of future research. It must be noted, that for $n = 3$ the classical barycentric coordinates produce negative weight deficiency; nevertheless, 3-sided patches work nicely—see the examples. In this case, the middle control point is supposed to be set either by the default algorithm (Section 4.4) or by interpolating a prescribed middle surface point (Section 5.3). In order to ensure positive weight deficiency for triangular surfaces, our recommendation is a simple reparametrization of the distance coordinates, similarly to the one suggested in [SVR14].

The GB patch can be used with linear and quadratic boundaries, as well. In these cases there is only a single layer of control points, so C^0 continuity is guaranteed, and the scheme remains valid.

The extension of the GB scheme to higher degree ribbons and G^2 continuity, and the use of incompatible twists are subject of ongoing research; results are encouraging.

For the majority of practical applications it is sufficient that the

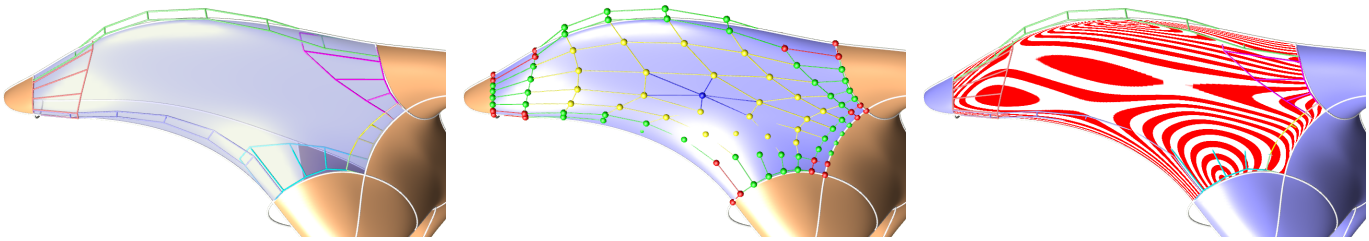

(a) Ribbons (b) Control points (c) Isophotes

Figure 12: Close-up of a 6-sided patch.

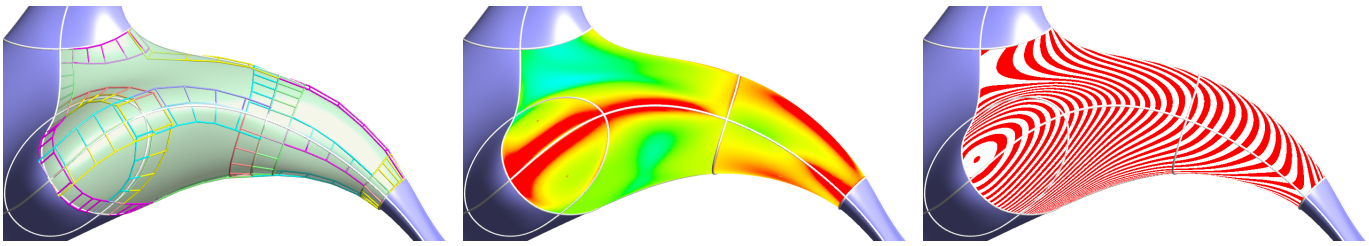

(a) Ribbons (b) Mean curvature (c) Slicing

Figure 13: Close-up of connected patches.

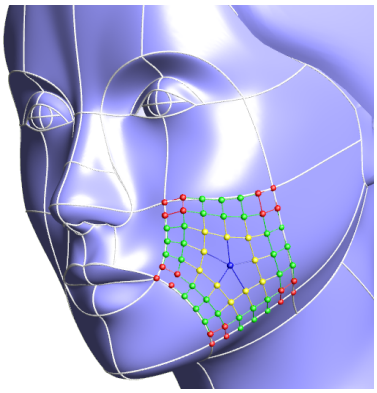

Figure 14: The face model.

GB patch intuitively interpolates the ribbons and produces a predictable middle surface point, but from a mathematical point of view it is a deficiency that this sort of degree elevation cannot reproduce the original degree $d-1$ patch. Our experiments show that good approximations by manual editing are possible; still, this is expected to be solved by an optimization algorithm. It is an open question whether a scheme with perfect degree elevation exists.

The GB scheme, as all control point based schemes, is suitable for fairing by minimizing various smoothness functionals, tweaking primarily the control points in the interior. Other sorts of optimizations are also possible, including the approximation of given point sets while the boundaries are constrained. These algorithms are subject of future research, as well.

Conclusion

A new multi-sided surface scheme has been proposed that generalizes tensor product Bézier patches, based on the displacement principle. The control net seems to be the simplest extension of conventional quadrilateral grids. GB patches combine Bézier ribbons with different degrees, and build up a uniform structure with automatically produced interior control points. This is accomplished by special degree elevation and degree reduction algorithms. There exists an extra degree of freedom to set the middle point of the patch, if needed.

GB patches use rationally weighted biparametric Bernstein functions; this explains why the most important properties of tensor product Bézier patches remain valid. The patches have internal C^∞ continuity, it is easy to evaluate them and are well-suited for a GPU implementation. GB patches are expected to be used in various computer graphics and CAD applications including interactive general topology curve network-based design, hole filling, reverse engineering and surface approximation. There are lots of challenging open issues for future research.

Acknowledgments

This is a joint work by researchers at the Budapest University of Technology and Economics and a small technology company ShapEx Ltd., Budapest. The pictures were generated by a prototype system called Sketches. The dolphin model has been provided for us by Cindy Grimm (Washington University); the face model was designed by Supriya Chewle (KAUST, Saudi Arabia). The project was partially supported by the Hungarian Scientific Research Fund (OTKA, No. 101845).

References

[Coo67] COONS S. A.: *Surfaces for Computer-Aided Design of Space Forms*. Tech. Rep. MIT/LCS/TR-41, Massachusetts Institute of Technology, 1967. 2

[Gre86] GREGORY J. A.: N-sided surface patches. In *Mathematics of Surfaces I* (1986), Oxford University Press, pp. 217–232. 2

[GZ94] GREGORY J. A., ZHOU J.: Filling polygonal holes with bicubic patches. *Computer Aided Geometric Design 11*, 4 (1994), 391–410. 2

[HF06] HORMANN K., FLOATER M. S.: Mean value coordinates for arbitrary planar polygons. *Transactions on Graphics 25*, 4 (2006), 1424–1441. 3

[HK84] HOSAKA M., KIMURA F.: Non-four-sided patch expressions with control points. *Computer Aided Geometric Design 1*, 1 (1984), 75–86. 2

[KNP15] KARČIAUSKAS K., NGUYEN T., PETERS J.: Generalizing bicubic splines for modeling and IGA with irregular layout. *Computer-Aided Design* (2015). 2

[LD89] LOOP C. T., DEROSE T. D.: A multisided generalization of Bézier surfaces. *Transactions on Graphics 8* (1989), 204–234. 2

[LS08] LOOP C., SCHAEFER S.: G^2 tensor product splines over extraordinary vertices. In *Computer Graphics Forum* (2008), vol. 27, Wiley Online Library, pp. 1373–1382. 2

[Mal98] MALRAISON P.: A bibliography for n-sided surfaces. In *Mathematics of Surfaces VIII* (1998), Information Geometers, pp. 419–430. 2

[Pet94] PETERS J.: Constructing C^1 surfaces of arbitrary topology using biquadratic and bicubic splines. In *Designing Fair Curves and Surfaces: Shape Quality in Geometric Modeling and Computer-Aided Design*. Society for Industrial and Applied Mathematics, 1994. 2

[Pra97] PRAUTZSCH H.: Freeform splines. *Computer Aided Geometric Design 14*, 3 (1997), 201–206. 2

[Sab83] SABIN M.: Non-rectangular surface patches suitable for inclusion in a B-spline surface. In *EuroGraphics* (1983), North Holland, pp. 57–70. 2

[SS15] SMITH J., SCHAEFER S.: Selective degree elevation for multi-sided Bézier patches. *Computer Graphics Forum 34*, 2 (2015), 609–615. 2

[SVR14] SALVI P., VÁRADY T., ROCKWOOD A.: Ribbon-based transfinite surfaces. *Computer Aided Geometric Design 31*, 9 (2014), 613–630. 1, 2, 9

[SZ15] SUN L.-Y., ZHU C.-G.: G^1 continuity between toric surface patches. *Computer Aided Geometric Design 35–36* (2015), 255–267. Geometric Modeling and Processing 2015. 2

[VRS11] VÁRADY T., ROCKWOOD A., SALVI P.: Transfinite surface interpolation over irregular n-sided domains. *Computer Aided Design 43*, 11 (2011), 1330–1340. 2

[War92] WARREN J.: Creating multisided rational Bézier surfaces using base points. *Transactions on Graphics 11* (1992), 127–139. 2

[ZB97] ZHENG J., BALL A.: Control point surfaces over non-four-sided areas. *Computer Aided Geometric Design 14*, 9 (1997), 807–821. 2

[Zhe01] ZHENG J.: The n-sided control point surfaces without twist constraints. *Computer Aided Geometric Design 18*, 2 (2001), 129–134. 2